Journal of Scientific Research & Reports
11(2): 1-9, 2016; Article no.JSRR.26362
ISSN: 2320-0227

SCIENCEDOMAIN *international*
www.sciencedomain.org

Production of Low Electron-Temperature and High Density Plasma by Using a Grid-Cage Electrode for RF Discharge

Kohgi Kato[1], Takuma Gohda[1] and Satoru Iizuka[1*]

[1]Department of Electrical Engineering, Graduate School of Engineering, Tohoku University, Aza Aoba 6-6-05, Aramaki, Aoba-ku, Sendai 980-8579, Japan.

Authors' contributions

This work was carried out in collaboration between all authors. Author SI proposed the study and the experiment was carried out by author KK, in discussion with authors TG and SI. All data were acquired and processed by author KK. The results were discussed with all authors and the first draft of the manuscript was written by author KK. All authors approved the final manuscript.

Article Information

DOI: 10.9734/JSRR/2016/26362
Editor(s):
(1) Cheng-Fu Yang, Department of Chemical and Materials Engineering, National University of Kaohsiung, Kaohsiung, Taiwan.
Reviewers:
(1) Gamal G. Elaragi, Nuclear Research Center, Cairo, Egypt.
(2) Kamal M. Ahmed, Nuclear Research Centre, Atomic Energy Authority, Egypt.
(3) Stanislav Fisenko, Moscow State Linguistic University, Russia.
Complete Peer review History: http://sciencedomain.org/review-history/14926

Original Research Article

Received 13th April 2016
Accepted 31st May 2016
Published 7th June 2016

ABSTRACT

An original method for producing low electron temperature and high electron density plasma was studied experimentally by using a rectangular grid-cage as a capacitively-coupled powered electrode in a radio frequency (RF) discharge.
A rectangular grid-cage electrode was placed on a side wall of a grounded cubic-box chamber of $15 \times 15 \times 15\ \mathrm{cm}^3$ in volume. The cubic chamber was situated in a stainless steel vacuum chamber 60 cm in diameter and 100 cm long. An argon plasma was generated by a 40 MHz power source in a pressure range of 2.0 ~ 6.7 Pa. RF power P_{RF} of $5 \sim 60$ W was supplied to the grid-cage electrode directly through an impedance matching circuits with a dc blocking capacitor for efficient plasma production.
The electron temperature T_{e} and electron density n_{e} were found to be strongly dependent on a mesh size of grid-cage electrodes. If the mesh of the grid-cage was fine, T_{e} decreased, while n_{e} increased, compared with those in the case of a coarse grid-cage electrode. By using a fine grid-

**Corresponding author: E-mail: iizuka@ecei.tohoku.ac.jp;*

electrode, T_e dropped down to 0.5 eV, while n_e reached up to 1.62×10^{11} cm^{-3} at the center of the cubic discharge chamber of $15 \times 15 \times 15$ cm^3 under argon pressure of 2.0 Pa and RF power of 60 W.
This discharge method easily provides low electron temperature and high density plasmas under the continuous RF discharge.

Keywords: Low electron-temperature plasma; high density plasma; low space potential; grid-cage electrode; RF discharge.

1. INTRODUCTION

Currently, the studies on a production of low electron temperature and high electron density plasmas have been energetically proceeded in order to establish negative ion plasma source for neutral beam injection (NBI) in the fusion devices [1,2]. Further, also in the semiconductor device fabrication, NBI method has been used extensively as an important plasma-free technology for ultra-fine etching processing [3], thin film deposition [4], and so on. For producing a neutral beam, a technique to generate a high density negative ion plasma is required. As is well known, in order to produce negative ions efficiently, it is necessary to generate high density plasma with low electron temperature for an efficient electron attachment.

By using such low electron temperature plasma, several methods have been reported for producing negative ion plasmas [1-7]. N. Hershkowitz and T. Intrator created a two-component plasma with negative ions SF_6^- and positive ions Ar^+ in a mixed gas of SF_6 and Ar at the downstream of the magnetic filter [5], although the density of plasma dropped off one decade during passage through the magnetic filter. M. B. Hopkins and K. N. Mellon made use of a pulsed discharge methode for generation of negative hydrogen ions [7]. They observed negative ions in the low-density plasma after the discharge was stopped.

We also reported a grid-bias technique which yielded a continuous decrease of T_e and an increase of n_e by applying negative direct current (dc) voltage V_G to a mesh grid which separates the plasma into two regions [8-11]. With a decrease in V_G from -5 V to -15 V, there appears a clear drop of T_e from 2.1 eV to 0.035 eV, which is accompanied by an increase in n_e [10]. The ion temperature T_i is also lowered by changing T_e [12]. A production of high density ($= 2 \times 10^{11}$ cm^{-3}) and low electron temperature ($= 0.3$ eV) plasma was realized by modified grid-biasing method using inductively coupled RF discharge at 200 W [13]. Although the grid is covered with a thin film made of a diamond-like carbon known as an insulating material, the grid bias method can still control the electron tmeperature over a wide range [14]. Also, another method using a grid for T_e control was proposed. In this method, T_e is controlled by varying mechanically the length of slits in a plasma [15]. This technique was applied to the production of high-quality diamond prepared in an RF discharge CH_4/H_2 plasma [16]. In the depositon experiment, the sample grown in the high electron temperature ($= 2.24$ eV) plasma was mainly amorphous graphite. On the other hand, the film grown in the low electron temperature ($= 0.52$ eV) plasma was indeed diamond.

Up to now, a few important studies on the production of negative ion plasma using a grid-bias method have been performed [17-20]. We observed that the negative to positive saturation probe current ratio I^-/I^+ was reduced markedly from 28 to 1.2 as the grid bias voltage decreased from 30 to -15 V in pure hydrogen gas [17]. This result suggests the effective generation of negative hydrogen ions due to a reduction of the electron temperature. O. Fukumasa et al. investigated a comparison between the grid-bias method and magnetic filter method [20]. They confirmed that in the case of an RF discharge plasma the grid bias method was more suitable to optimize plasma conditions for negative ions, compared with the magnetic filter method.

In the future, the plasma production of low electron temperature (≤1 eV) and high density ($\sim 2 \times 10^{11}$ cm^{-3}) at the low power of 100 W will be strongly desired for qualified plasma processings. In this paper, we present a novel plasma source with a performance described above by employing capacitively-coupled continuous RF discharge with a use of a rectangular grid-cage electrode.

2. EXPERIMENTAL SETUP AND MEASUREMENT

2.1 Experimental Device

Fig. 1 shows a schematic of the experimental apparatus. A rectangular grid-cage electrode is placed on a side wall of a grounded cubic-box chamber of $15 \times 15 \times 15\ \mathrm{cm}^3$ in volume. The cubic chamber is situated in a stainless steel vacuum chamber 60 cm in diameter and 100 cm in length, which is evacuated to a pressure of 0.3 Pa by using a rotary pump. Since the outer wall of the cubic chamber is grounded electrically, the discharge turns on only inside the cubic chamber. The gas pressure is measured by a Pirani gauge. An argon plasma is generated by a 40 MHz power source in a pressure range of 2.0 ~ 6.7 Pa (15 ~ 50 mTorr). The plasma produced in our experiment was not exactly pure argon plasma. But, in application to the plasma processing, the working reactive gas is often molecular gas with Ar as dilution gas. In this experiment one can regard that the molecular air gas is diluted by Ar. RF power P_{RF} of $5 \sim 60$ W is supplied to the grid-cage electrode directly through an impedance matching circuits with a dc blocking capacitor for efficient plasma production. Usual 13.56 MHz will also be available in our experiment. Here, electric power was measured and displayed on a panel of the RF generator.

2.2 Electrodes for RF Discharge

We used three types of RF electrode in our experiment. The first one (Type A) is a flat plane electrode made of aluminum with a surface area of $5 \times 5\ \mathrm{cm}^2$ and a thickness of 0.1 cm. A mica plate with the same area and thickness as Type A electrode is sandwiched between this plane electrode and a wall of the cubic chamber. These plates are not shown in Fig. 1. The second one (Type B) is a rectangular grid-cage electrode made of stainless steel as shown by a dotted line in Fig. 2. Back and side surfaces of this grid-electrode are covered with mica plates of 1 mm each in thickness, which are also covered with grounded aluminum plates in 1 mm thickness for electrical shielding. The back area and height of Type B electrode are $5 \times 5\ \mathrm{cm}^2$ and 1 cm, respectively. The mesh size and wire diameter of Type B are 1.97 mesh/cm and 0.5 mm, respectively. The third one (Type C) is also a grid-electrode which dimensions and shape are the same as those of Type B, but the mesh size and wire diameter of Type C electrode are 6.3 mesh/cm and 0.29 mm, respectively.

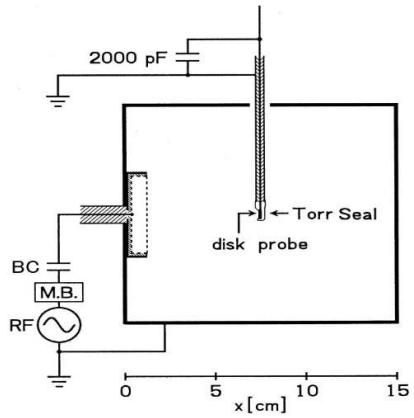

Fig. 1. Schematic of the experimental apparatus for a production of low electron temperature T_{e} and high density n_{e} plasmas

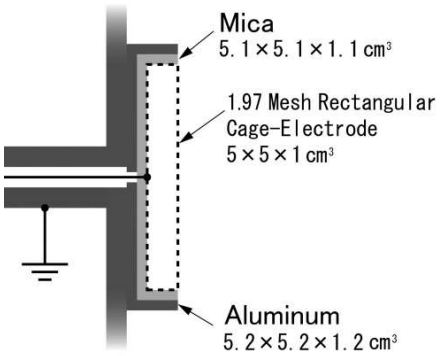

Fig. 2. Diagram of the rectangular grid-cage electrode

2.3 Measurement Method of Plasma Parameters

The plasma parameters are measured by a single probe (diameter 3 mm, thickness 0.3 mm) made of tantalum disk. The probe disk is welded to a copper core wire of a 50 Ω semi-rigid coaxial-cable (outer diameter 2.2 mm), which is sleeved with a glass fiber tube. One side of the probe disk is used as a collector of the probe current, and the other surface is covered with Torr Seal which is a sealant made of low vapor pressure resin. In our experiment, this sealant did not deteriorate even in high-density plasmas because of the low electron temperature. The origin of the *x*-axis is set at the wall (x = 0 cm) of the cubic-box chamber, in which the grid-cage electrode is placed as shown in Fig. 1. The probe

disk is set at x = 2.5 cm or 7.5 cm. A ceramic capacitor of 2,000 pF is connected in parallel to the probe circuit in order to remove effects of RF potential fluctuations causing a fatal error to the plasma parameters, so that the dc current only flows through the measuring circuit. The semi-rigid cable described above is connected to a 3D-2V coaxial cable by a BNC connector outside of the vacuum chamber. The 3D-2V cable is also connected to Source Meter-2400 manufactured by Keithley Instruments. The probe current I_p was measured at the probe voltage V_p supplied by Source Meter-2400. Before drawing each current-voltage (I_p - V_p) trace the probe surface continued to be cleaned up by bombarding of ions applied a negative voltage of -150 V for 20 s. The values of the dc probe current I_p and voltage V_p collected through Source Meter-2400 are stored on the personal computer, and at the same time, a probe characteristic curve is drawn automatically on the display of the computer using the software that we have created using Microsoft Visual C++. By using this software plasma parameters are also determined easily from a semi-log plot of an electron current I_e which is obtained from a probe characteristic curve. The method for probe measurement of plasma parameters in RF discharge [21-23] was explained in detail in Ref. [24].

3. EXPERIMENTAL RESULTS

3.1 T_e and n_e Versus P_{RF} for Three Different Electrodes

First, three RF electrodes are compared under the same experimental conditions. Fig. 3 shows dependencies of electron temperature T_e and electron density n_e on RF power P_{RF} for three different electrodes, i.e. a plate (Type A) and rectangular grid-cages of two different mesh sizes which are 1.97 mesh/cm (Type B) and 6.3 mesh/cm (Type C). Argon gas pressure P_{Ar} is 4.0 Pa (= 30 mTorr) and the probe position is fixed at x= 2.5 cm. As shown in Fig. 3(a), in the cases of the grid-cage electrodes, the electron temperature is gradually decreased with an increase in P_{RF}. Electron temperature T_e becomes 1.7 eV and 0.9 eV at 60 W in the cases of the coarse (Type B) and fine (Type C) mesh electrodes, respectively.

On the other hand, T_e simply rises up from 1.4 eV to 3.4 eV as P_{RF} increases from 5 W to 60 W for the plate electrode (Type A). Fig. 3(b) shows dependencies of n_e on P_{RF}. The density obtained by using the plate electrode is 5×10^9 cm^{-3} at 30 W. This density is comparable to that obtained in the normal capacitively-coupled RF discharge plasma [19]. On the other hand, when the grid-cage electrodes are employed, it is shown that in the case of the grid electrode of 1.97 mesh/cm (Type B), n_e is roughly ten times higher than that in the case of the plate electrode over a whole range of P_{RF}. It is also shown that T_e in the case of Type C is reduced compared to that of Type B. And, n_e in the case of Type C is much larger than that of Type B. Both of the electron temperature and electron density are dependent on the mesh size of the grid. In other words, T_e can be reduced and n_e can be increased by employing a finer mesh electrode. Therefore, the grid-cage electrode of 6.3 mesh/cm (Type C) is most suitable for a low electron temperature and high density plasma source.

3.2 T_e, n_e and V_s Versus P_{RF} for Type C Electrode

Next, the performance of Type C electrode is investigated in a lower pressure regime. Fig. 4 shows dependencies of the plasma parameters on RF power P_{RF} under Ar pressure $P_{Ar} = 2.7$ Pa (= 20 mTorr) for Type C electrode. The probe positions in Figs. 4(a) and 4(b) are x = 2.5 cm and 7.5 cm, respectively. In the case of x = 2.5 cm, the electron density n_e increases to 2.6×10^{11}cm^{-3} at $P_{RF} = 60$ W. The density n_e at x = 2.5 cm is roughly two times higher than that at x = 7.5 cm. T_e is gradually decreases with an increase of P_{RF} in the range between 5 W and 30 W. But it shows constant value 0.6 eV at $P_{RF} \geq 30$ W. This feature of T_e will be discussed in section 4. It is also shown that T_e and time-averaged space potential V_s are independent of the probe position x. Here, V_s shows a low value of 15.5 V due to the low electron temperature of 0.6 eV.

3.3 T_e, n_e and V_s versus P_{Ar} for Type C Electrode

In order to investigate pressure dependence of the plasma parameters in the case of Type C electrode, T_e, n_e and V_s are measured at RF power of $P_{RF} = 60$ W and x =7.5 cm as a function of argon pressure P_{Ar} as shown in Fig. 5 for the case of the fine grid-cage electrode (6.3 mesh/cm, Type C). T_e increases from 0.5 eV to 1.4 eV, while n_e decreases from 1.6×10^{11}cm^{-3} to 0.35×10^{11}cm^{-3} as P_{Ar} rises from 2.0 Pa to 6.7 Pa. These dependencies differ from those of usual RF plasmas [25]. In addition, V_s can be kept low, i.e. 13.2 V at 2.0 Pa, due to the

decrease of T_e, so that ion bombardments can be suppressed. Therefore, this grid cage electrode is very useful for a damage-free processing plasma source.

It is also found that V_s is kept almost constant when the RF power is increased. This is convenient because the sheath potential in front of the substrate placed in the plasma does not vary during the film deposition, for example. However, as shown in Fig. 5, V_s increases gradually with an increase in Ar pressure, i accordance with the increase in the electro temperature.

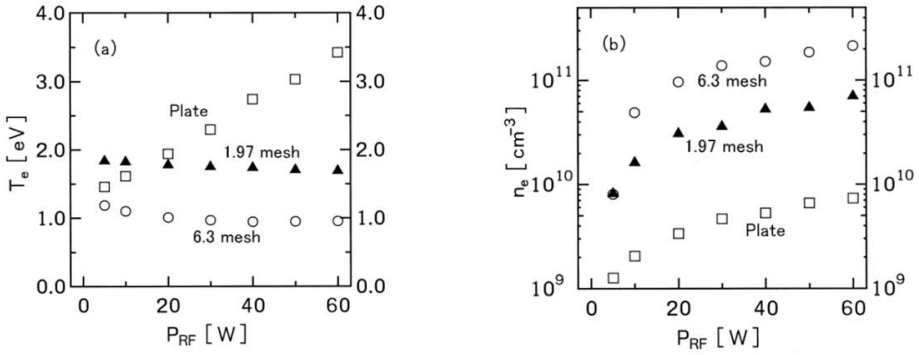

Fig. 3. Dependencies of (a) T_e and (b) n_e on P_{RF} for various electrodes. x = 2.5 cm and P_{Ar} = 4.0 Pa

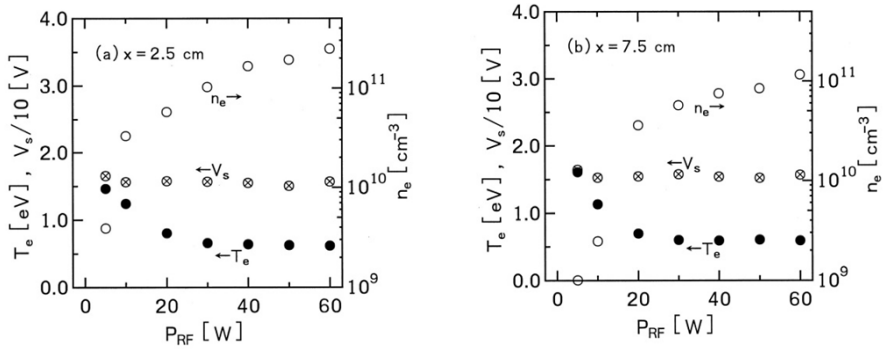

Fig. 4. Dependencies of the plasma parameters (T_e, n_e and V_s) on P_{RF} for Type C electrode. $P_{Ar} = 2.7$ Pa. (a) x = 2.5 cm and (b) 7.5 cm

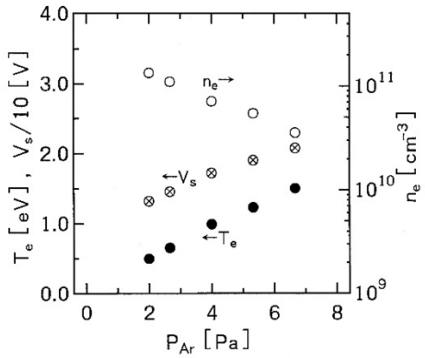

Fig. 5. Dependencies of the plasma parameters (T_e, n_e and V_s) on P_{Ar} for the fine mesh electrode (Type C). x = 7.5 cm and $P_{RF} = 60$ W

3.4 Spatial Variation of Plasma Parameters for Type B Electrode

Measurement of spatial profiles of plasma parameters is important for considering a mechanism of the production of low electron temperature plasma outside the grid cage. Especially, in order to investigate a role of plasma produced inside the grid cage, spatial variations of n_e, T_e, and V_s are measured through the grid for Type B electrode, as shown in Fig. 6. Here, the grid position is shown by a dotted line. The *x* coordinate is defined in Fig. 1. In Fig. 6 it is remarkable that the temperature T_e inside the grid cage is found to be about 4.3 eV, which is higher than 1 eV outside the grid cage. The value of 4.3 eV is quite similar to that in normal RF discharge plasmas. The density n_e at *x* = 2.5 cm (outside) is about three times higher than that at *x* = 0.5 cm (inside). Conversely, V_s at *x* = 2.5 cm (outside) is lower than that at *x* = 0.5 cm (inside). It will be explained in section 4 that this potential distribution is very important for producing the low T_e and high n_e plasma in the outside of the grid.

3.5 T_e, n_e and V_s versus P_{Ar} for Type B Electrode

The plasma parameters inside and outside of the grid cage are shown in Fig. 7(a) and 7(b), respectively, as a function of argon pressure P_{Ar} for the case of Type B electrode (1.97 mesh/cm). The probe positions of Fig. 7 (a) and (b) are *x* = 0.5 cm (inside) and 3.5 cm (outside), respectively. It is remarkable that T_e inside the grid cage decreases with an increase in P_{Ar}, although T_e outside the grid cage increases with an increase in P_{Ar}. Conversely, n_e inside the grid cage increases with an increase in P_{Ar}, although n_e outside the grid cage decreases with an increase in P_{Ar}. On the other hand, the plasma potential V_s increases gradually with increasing P_{Ar}, although V_s variation inside the grid cage is small.

The behaviors of plasma parameter dependences outside the grid cage are quite different from those inside the grid cage. The pressure dependences of the plasma produced inside the grid cage are similar to those of usual RF plasmas [25].

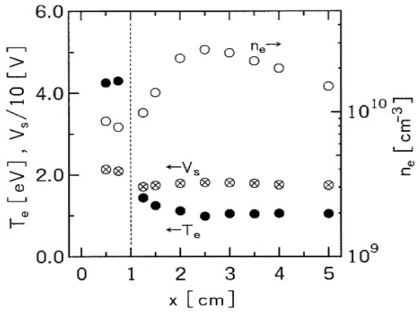

Fig. 6. Spatial (*x*) variations of T_e, n_e and V_s for Type B electrode. The grid electrode position is shown by a dotted line. $P_{Ar} = 2.7$ Pa and $P_{RF} = 20$ W

4. DISCUSSION

Distances between the grid wires of Type B and C are 4.58 mm and 1.29 mm, respectively, so that the estimated grid transparencies are 81.3% and 66.8%, respectively. In the case of $T_e = 1$ eV and $n_e = 10^{10}$ cm^{-3}, the Debye length $\lambda_D = 740(kT_e/n_e)^{1/2}$ is estimated to be about 0.075 mm. Thus, the grid wire distance is much larger than the Debye length. Therefore, the space between the wires is enough for the electrons to pass through the grid.

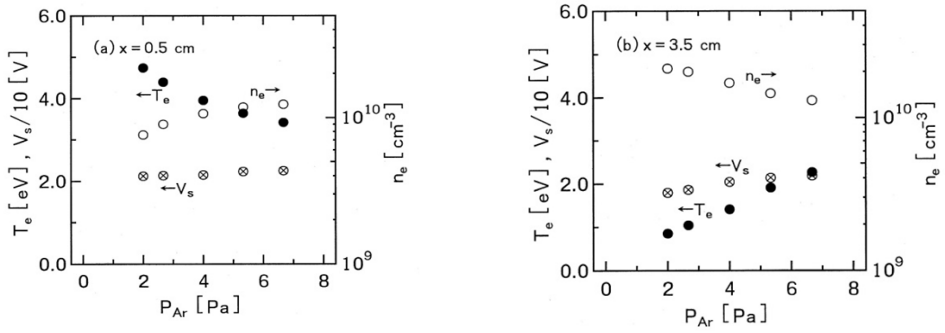

Fig. 7. Comparison of T_e, n_e and V_s between (a) inside (*x* = 0.5 cm) and (b) outside (*x* = 3.5 cm) of the coarse mesh electrode (Type B) as a function of P_{Ar} at $P_{RF} = 20$ W

Since the grid cage has a space inside, the plasma production takes place not only outside but also inside the grid-cage electrode. Actually, we observed high electron temperature plasmas inside the grid cage and low electron temperature plasmas outside the grid cage, as shown in Figs. 6 and 7. These two plasmas are separated by the grid cage between these plasmas. Fig. 8 shows RF self-bias dc voltage V_{dc} evolved on the Type C electrode as a function of RF power in the case of Fig. 4. It is noted that V_{dc} is negative and lowered simply from -35 V to -82 V as P_{RF} is increased from 10 W to 60 W, while V_{s} outside the grid cage is almost constant at +16 V (see Fig. 4). Since V_{s} inside the grid cage is also positive and higher than that outside the grid cage (see Figs. 6 and 7), the negatively biased grid cage potential $V_{\mathrm{dc}}(<0)$ electrically separates the high energy electrons inside from the low energy electrons outside, acting as a thermal barrier [26-29].

With an increase in the RF power the self-bias voltage V_{dc} of the grid becomes more negative and suppresses the high energy electrons flowing from the inside to the outside. However, since the grid potential oscillates in time, the high energy tail of electrons can have a chance to pass through the grid from the inside to outside and act as primary electrons for ionization outside the grid cage. The electrons generated by such ionization outside the grid cage would not get more energy because the space potential outside the grid cage is nearly homogeneous as shown in Fig. 6. Therefore, the bulk electron temperature outside the grid cage can be kept low. Moreover, these low temperature electrons are well confined electrostatically due to negative sheath potential surrounding the low electron temperature plasma (see Fig. 6). Therefore, the low energy electron confinement becomes better, then its density becomes relatively high. Note that the high energy tail of electrons passing though the grid are observed to decay within 5 mm from the grid position due to ionization [10], and the electrons in the other region outside the grid are regarded as a single Maxwellian. The electron density also increases with an increase in RF power.

As shown in Fig. 6 the electron temperature inside the grid cage is rather high, similar to the conventional RF plasmas. Therefore, when the confinement of such high temperature electrons is weakened, high temperature bulk electrons can leak into the outside. Then, the electron temperature outside the grid cage increases.

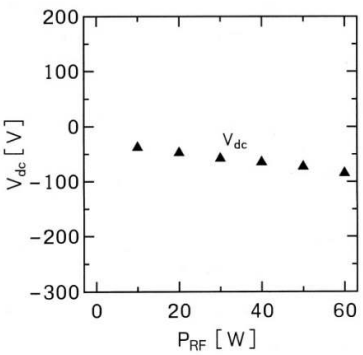

Fig. 8. Dependencies of self-bias dc voltage $\mathbf{V_{dc}}$ on RF power $\mathbf{P_{RF}}$ for Type C electrode. $\mathbf{P_{Ar} = 2.7}$ Pa. The experimental condition is the same as Fig. 4

The important point in this case is not only negative self-bias voltage induced on the surface of grid wires, but also a confinement of bulk electrons inside the grid cage by the grid potential. The increase of electron temperature outside the grid cage can be explained by the loss of such high energy bulk electrons confined inside the grid toward the outside. There exist three ways to increase the electron temperature outside the grid cage. The first one is to use a coarse grid. Actually, when the coarse grid is employed, the electron temperature outside the grid increases as shown in Fig. 3. The second one is to diminish the negative potential barrier V_{dc} by lowering the input power (see Fig. 8). Actually, the electron temperature increases with a decrease in RF power as shown in Fig. 4. The third one is to increase collisions between the electrons and Ar atoms by increasing Ar pressure. The effect of electrostatic electron trapping within the grid cage will be weakened by increasing the collisions. In fact, as shown in Fig. 5 and 7(b), the electron temperature outside the grid-cage electrode raises with an increase in Ar pressure. Simultaneously, the electron density is decreased due to an increase in the electron loss toward the wall. On the contrary, T_{e} inside of the grid cage is decreased with an increase in P_{Ar}. This is thought to be due to a collisional cooling, as in the conventional discharges.

As explained above, trapping of high energy electrons produced inside the grid cage electrode is very important for producing low electron temperature plasma outside the grid cage. As shown in Figs. 3 and 4 the electron temperature was simply decreased with an increase in the RF input power in the cases of Type B and C

electrodes. Conversely, the electron temperature increased with an increase in the RF power in the case of the plate electrode (Type A). The biggest difference between Type A and C (or B) comes from the effect of electron trapping in the grid-cage electrode. The plate electrode behaves as if in a limit of the grid with zero transparency.

It is noted that such low T_e and high n_e plasma mentioned above is also generated even when the back side of the grid cage shown in Fig. 2 is replaced by an aluminum plate. We have already succeeded in generation of a low electron-temperature and high electron density plasma.

Since the low electron temperature and high electron density RF plasmas are produced by a grid cage electrode discharge, this technique will be applied to an efficient production of negative ion plasmas, which are widely used in fusion plasma heating and material processing by a neutral beam injection.

5. CONCLUSION

We have developed a novel method for generating a low electron temperature and high density plasma by using a capacitively-coupled continuous RF discharge with a powered grid-cage electrode. In the case of the mesh electrode of 16 mesh per inch (Type C), for example, T_e dropped down to 0.5 eV, while n_e reached up to 1.5×10^{11} cm^{-3} at $P_{Ar} = 2.0$ Pa and $P_{RF} = 60$ W at the center of the discharge chamber. Unlike normal RF discharge plasmas, T_e increased and n_e reduced with an increase in P_{Ar} under a constant RF power. The phenomena are able to be explained by electron generation and trapping inside the grid cage. Conversely, when the plate electrode was used, T_e increased with RF power and a very low density plasma was produced.

Grid-cage electrode method is quite simple and available for a production of low electron temperature and high density plasma under the continuous RF discharge.

DISCLAIMER

This manuscript was presented in the conference "Conference Program 8th International Conference on Reactive Plasmas and 31st Symposium on Plasma Processing" available link is "http://plasma.ed.kyushu-u.ac.jp/~icrp-8/files/Scientific Program.pdf", date February 4-7, 2014, Place: Fukuoka International Congress Center, Fukuoka, Japan.

COMPETING INTERESTS

Authors have declared that no competing interests exist.

REFERENCES

1. Fants U, Franzen P, Kraus W, Falter HD, Barger M, Christ-Koch S, Fröschle M, Guster R, Heinemann B, Martens C, McNeely P, Riedl R, Speth E, Wünderlich D. Low pressue and high power rf sources for negative hydrogen ions for fusion applications (ITER neutral beam injection) (invited). Rev. Sci. Instrum. 2008;79: 02A511-1– 02A511-6.
2. Vozniy OV, Yeom Y. High-energy negative ion beam obtained from pulsed inductively coupled plasma for charge-free etching processes. Appl. Phys. Lett. 2009;94: 231502-1– 231502-3.
3. Samukawa S, Sakamoto K, Ichiki K. Generating high-efficiency neutral beams by using negative ions in an inductively coupled plasma source. J. Vac. Sci. Technol. 2002;A20(5):1566-1573.
4. Kikuchi Y, Wada A, Kurotani T, Nakano M, Inoue KY, Matsue T, Nozawa T, Samukawa S. Conductive amorphous hydrocarbon film for bio-sensor formed by low temperature neutral beam enhanced chemical vapor deposition. Charbon. 2014;67:635-642.
5. Hershkowitz N, Intrator T. Improved source of cold plasma electrons and negative ions. Rev. Sci. Instum. 1981;52(11):1629-1633.
6. Stamate E, Draghici M. High electro-negativity multi-dipolor electron cycrotron resonance plasma source for etching by negative ions. J. Appl. Phys. 2012;111: 083303-1– 083303-6.
7. Hopkins MB, Mellon KN. Enhanced production of negative ions in low-pressure hydrogen and duterium discharges. Phys. Rev. Lett. 1991;67:449-452.
8. Iizuka S, Koizumi T, Takada T, Sato N. Effect of electron temperature on negative hydrogen ion production in a low-pressure Ar discharge plasma with methane. Appl. Phys. Lett. 1993;63(12):1619-1621.
9. Kato K, Iizuka S, Sato N. Electron-tempeature decrease in an RF discharge plasma, in Proc. 10th Symp. Plasma Processing. Jap. Soci. Appl. Phys. 1993;353-356.

10. Kato K, Iizuka S, Sato N. Electron-temperature control for plasmas passing through a negatively biased grid. Appl. Phys. Lett. 1994;76:816-818.
11. Hong JI, Seo SH, Kim SS, Yoon NS, Chang CS, Chang HY. Electron temperature control with grid bias in inductively coupled argon plasma. Phys. Plasmas. 1999;6:1017-1028.
12. Kato K, Iizuka S, Sato N. Ion-energy control in a low elctron-temperature plasma, in Proc. 13th Symp. Plasma Processing, Jap. Soci. Appl. Phys. 1996;183 - 186.
13. Ikada R, Nishimure G, Kato K, Iizuka S. Production of high density and low electron-temperature plasma by a modified grid-biasing method using inductively coupled RF discharge. Thin Solid Films. 2004;457:55-58.
14. Kato K, Emi J, Iizuka S. Control of electron temperature by varying DC voltage to a mesh grid blanketed with thin film in plasmas. Jpn. J. Appl. Phys. 2008;47: 8565-8569.
15. Kato K, Iizuka S, Sato N. Electron temperature control by varying size of slitsmade in agrid. Appl. Phys. Lett. 2000;76:547-549.
16. Shimizu T, Iizuka S, Kato K, Sato N. High quality diamond formation by electron temperature control in methane-hydrogen plasma. Plasma Sources. Sci. Technol. 2003;12:S21–S27.
17. Iizuka S, Kato K, Takahashi A, Nakagomi K, Sato N. Negative hidrogen ions produced by electron temperature control in an RF plasma. Jpn. J. Appl. Phys. 1997;36(Pt. 1, No. 7B):4551-4553.
18. Fukumasa O, Ito D, Jyobira Y. Electron temperature control in plasmas with mesh grid bias and its application to hydrogen negative ion production, in Proc. 11th International Symp. on Production and Neutralization of Negative Ions and Beams, American Insti. Phys. 2007;31-37.
19. Okada J, Nakao Y, Tauchi Y, Fukumasa O. Efficient negative ion production in rf plasmas using a mesh grid bias method. Rev. Sci. Instum. 2008;79:02A502-1–02A502-3.
20. Jyobira Y, Ito D, Fukumasa O. Enhancement of pure volume negative ion production using a grid bias method or a magnetic filter method. Rev. Sci. Instum. 2008;79:02A508-1- 02A508-4.
21. Kato K, Nakagawa Y, Sato N. Effects on probe characteristic of high-frequency potential oscillation, in Proc. 41st Autumnal Simp. on Discharge and Plasma Physics. Phys. Soc. Jap. 1986;230.
22. Kato K, Sato N. Probe characteristics in plasmas involving fluctuation-potential of high-frequency, in Proc. 42nd Autumnal Simp. on Discharge and Plasma Physics. Phys. Soc. Jap. 1987;139.
23. Kato K, Ono H, Iizuka S. Langmuir probe characteristics in plasmas involving periodic oscillations of space potential, in Proc. 25th Symp. on Plasma Processing. Jap. Soci. Appl. Phys. 2008;313-314.
24. Kato K, Iizuka S. To be published in J. Sci. Res. Reports; 2016.
25. Godyak VA. Electrical and plasma parameters of ICP with high coupling efficiency. Plasma Sources Sci. Technol. 2011;20:025004-1– 025004-7.
26. Kato K, Gohda T, Iizuka S. A novel method for a production of low electron temperature plasma by a grid cage RF discharge, in Proc. 30th Symp. on Plasma Processing. Jap. Soci. Appl. Phys. 2013; 121-122.
27. Coburn JW, Kay E. Positive-ion bombardment of substrates in rf diode glow discharge sputtering. J. Appl. Phys. 1972;43:4965-4971.
28. Kohier K, Coburn JW, Home DE, Kay E. Plasma potentials of 13.56-MHz rf argon glow discharges in a planar system. J. Appl. Phys. 1985;57:59-66.
29. Kato K, Iizuka S, Gangly G, Ikeda T, Matsuda A, Sato N. Electron and ion controls in a radio frequency discharge plasma with silane. Jpn. J. Appl. Phys. 1997;36(Part 1, No. 7B):4547-4550.

Peer-review history:
The peer review history for this paper can be accessed here:
http://sciencedomain.org/review-history/14926